CHEMISTRY OF MATERIALS

Article

pubs.acs.org/cm

Levitated Droplets as Model System for Spray Drying of Complex Oxides: A Simultaneous in Situ X-ray Diffraction/Raman Study

Jörg Radnik,*[,†] Ursula Bentrup,[†] Jork Leiterer,[‡] Angelika Brückner,[†] and Franziska Emmerling*[,‡]

[†]Leibniz-Institut für Katalyse e.V. an der Universität Rostock, Albert-Einstein-Str. 29a, 18059 Rostock, Germany

[‡]BAM Federal Institute for Materials Research and Testing, Richard-Willstätter-Str. 12, 12489 Berlin, Germany

ABSTRACT: Levitated droplets can model spray drying, a process which is poorly understood despite its industrial importance. Monitoring the drying process by simultaneous synchrotron X-ray scattering and Raman spectroscopy provides insights into the processes starting from the molecular species up to larger crystalline particles forming the stable system. In this study, slurries of two different phosphate-containing ammonium iron molybdates with different Fe/Mo ratios which are used as precursors for catalysts were exemplarily studied. Next to the phases containing highly condensed Keggin anions other phases of less condensed molybdates and phosphates were formed during the drying depending on the composition of the slurry and the drying time. To validate the capability of this experimental approach, the stable samples obtained after the drying in the levitator were compared with samples obtained after conventional spray drying and filtration of the precipitates. The results of comprehensive characterization (X-ray diffraction (XRD), Raman, attenuated total reflection Fourier transformation infrared spectroscopy (ATR-FTIR), inductively coupled plasma optical emission spectroscopy (ICP-OES)) indicate that the setup can be used to acquire reliable information on the processes during spray drying of complex oxides by using minimal amounts of material with volumes of several micro liters.

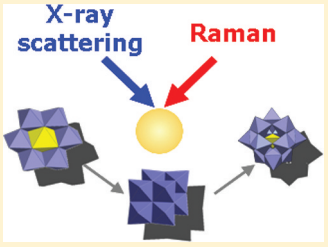

KEYWORDS: *synchrotron radiation, XRD, Raman spectroscopy, catalysts, iron molybdates, spray drying, acoustic levitation*

INTRODUCTION

Preparation of functional nanostructured inorganic materials with definite properties frequently comprises of series of subsequent steps such as precipitation of precursors, isolation of the precipitate, drying, and final calcination. Tailoring such multistep synthesis protocols for the reproducible and preferential formation of target phases is a true challenge, since a variety of parameters can have an influence.

Among others the drying process, that is, the transformation from a solution to a powder, plays an important role. Thus, it could be shown that this process is often accompanied by crystallization, which influences structure and morphology and, therewith, the performance of the final material.[1]

Spray drying is widely used in academia and industry for the production of thermal sensitive products as used in food and pharmaceutical industries or for the synthesis of inorganic solids with consistent particle size distribution used as catalyst materials.[2] Because of this importance efforts were made to get insights into the detailed processes going on during spray drying. One possibility is to change the spray drying conditions and to investigate the products ex situ with different analytical methods like X-ray diffraction or Scanning Electron Microscopy.[1,2] However, a more promising approach is the use of in situ techniques which allow a direct monitoring of the processes proceeding during spray drying. Scattering methods based on laser light or X-rays are suitable to follow the particle formation.[3] For inorganic compounds Small-Angle X-ray Scattering (SAXS) at synchrotron sources were used successfully.[1b,4] In these experiments particles which are formed in different zones of an oven were investigated providing information about the particle formation down to the sub nanometer region at different temperatures. A further possibility for the in situ monitoring of spray drying is to mimic conditions and processes as realized in the form of a levitated single droplet. Model predictions and experimental data for pharmaceutical relevant samples suggest the appropriateness of this model.[5] Because of a straightforward experimental setup this approach is advantageous and applicable for a wide spectrum of samples like proteins, inorganic salts, and organic compounds.[6] Additionally, this setup enables the experimental implementation of multiple analytical methods in parallel allowing the investigation of the proceeding processes on different length scales, from the molecular to the micro scale, under identical experimental conditions. Recently, some studies were published using coupled analytical techniques for the monitoring of particle formation and growth as well as phase transformation processes during the crystallization of pharmaceutical relevant materials in levitated droplets.[7] In these studies combined SAXS and X-ray absorption spectroscopy or X-ray diffraction (XRD) and Raman spectroscopy were used.

In contrast to polymers or pharmaceutical relevant materials, investigations relating to drying and crystallization of catalyst precursor materials are very rare, although catalysts are one prominent example of nanostructured materials often showing a great structural complexity. It was shown for complex Mo

Received: September 8, 2011
Revised: November 21, 2011
Published: November 21, 2011

oxides, that the catalytic performance is correlated with the drying method;[1a] however, systematic investigations of such drying processes are missing. Otherwise, preliminary investigations of the drying process of Mo-containing oxides in the acoustic levitator[8] were promising concerning the suitability of such experimental setup as model for spray drying.

In this paper we report on the monitoring of the drying process of catalyst precursor materials in an acoustic levitator by simultaneous synchrotron X-ray scattering and Raman spectroscopy. Two different phosphate-containing ammonium iron molybdate catalyst precursors with different Fe/Mo ratios were exemplarily studied to get information in terms of formation of crystalline phases and structural changes. For the experiments droplets of a slurry phase obtained by mixing ammonium heptamolybdate, iron nitrate, and phosphoric acid were injected into the ultrasonic levitator. To prove the concept of using levitated droplets as model for spray drying, the structural properties of samples obtained from the drying in the acoustic levitator and conventional spray dried powders of the same slurry phase were compared using different analytical methods like XRD, Raman spectroscopy, SAXS and Scanning Electron Microscopy (SEM). Additionally, the dried precipitates isolated from the slurries by filtration were investigated to get information about the influence of conditioning on phase composition and structure.

EXPERIMENTAL SECTION

Preparation. Two different slurries of 100 mL with different Mo/Fe ratios (**1-Fe**: 14, **2-Fe**: 12) were prepared by subsequent adding of iron(III) nitrate/HNO_3 solution and phosphoric acid (H_3PO_4) to an ammonium heptamolybdate (AHM) solution. In the first step the iron nitrate solution (4.04 g in 25 mL H_2O) was mixed with HNO_3 (1.3 mL) and then slowly added to the AHM solution (24.72/21.18 g of AHM in 75 mL of H_2O) at room temperature under continuous stirring. Subsequently, this mixture was stirred for 1 h at 25 °C. In the second step 1.3 mL of H_3PO_4 (85%, Aldrich) were added, followed by stirring for 30 min at 25 °C and further 60 min at 50 °C. After cooling to room temperature, a droplet of the obtained slurry phase was directly injected into the acoustic levitator.

For comparison the same procedure was applied and the obtained slurry phase was conventionally spray dried using a Mini Spray Dryer B-290 (BÜCHI). In a separate experiment the formed precipitate in the slurry phase was isolated by filtration, then washed with water and dried at ambient temperature.

Acoustic Levitation. An acoustic levitator (tec5 AG, Oberursel, Germany) was used as sample holder. Acoustic levitation is a versatile technique for sample handling where the levitated sample is only surrounded by the gaseous environment of air and any contact of the sample to solid surfaces is avoided. A detailed description of the experimental setup can be found in ref 9. In a typical experiment a droplet with a volume of about 4 μL was injected into the acoustic levitator with a common Eppendorf pipet (size 0.5−10 μL, Eppendorf, Germany). The sample remains in a fixed position during the measurement, even after complete evaporation of the solvent. The position stability of the droplet, measured as a displacement smaller than 20 μm, allowed more than 30 min of data acquisition time.

Raman Spectroscopy. The in situ Raman spectra were recorded directly from the levitated droplet using a fiber optical RXN-Spectrometer (Kaiser Optical Systems) equipped with a 70 mW diode laser for excitation at a wavelength of 785 nm. The laser beam was focused by a transmission optic onto the droplet with a spot diameter of 1 mm and a focal distance of 178 mm.

Attenuated Total Reflection (ATR) Spectroscopy. The ATR-FTIR spectra of the solid samples were measured using a Bruker Alpha FTIR spectrometer.

X-ray Diffraction (XRD). The in situ XRD experiments were performed at the synchrotron micro focus beamline (μSpot; BESSY II of the Helmholtz Centre Berlin for Materials and Energy). A detailed description of the beamline can be found in ref 10. The beamline is designed to provide a beam diameter of 20−100 μm at a photon flux of 1×10^9 s^{-1} at a ring current of 100 mA. The experiments were carried out employing a wavelength of 1.03358 Å. Scattered intensities were collected 230 mm behind the sample position with a two-dimensional X-ray detector (MarMosaic, CCD 3072 × 3072 pixel and a point spread function width of about 100 μm). The obtained scattering images were processed and converted into diagrams of scattered intensities versus scattering vector q (q is defined in terms of the scattering angle θ and the wavelength λ of the radiation, thus $q = 4\pi/\lambda \sin \theta$) employing an algorithm from the computer program FIT2D.[11] For the phase analysis the scattering vector was transformed into the commonly used 2θ-values obtained with Cu Kα radiation (λ = 1.5418 Å).

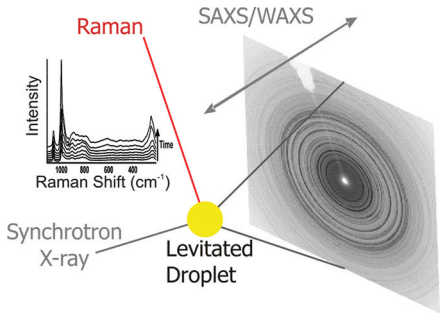

Figure 1. Scheme of the experimental setup installed around the levitated sample.

The applied experimental setup is schematically presented in Figure 1.

Detection of the Droplet Volume. The size of the levitated droplet and therefore its volume was observed in an additional experiment using its shadow. A distinct shadow-graph of the droplet was shaped by illumination with a telecentrically infrared flash light and recorded by CCD camera on the opposite side of the droplet. The shadowing is due to the strong absorption of the solvent (water) in this infrared region (λ = 880 nm). Details on the setup and the size determination can be found elsewhere.[12]

RESULTS AND DISCUSSION

The drying process of the two slurry samples with Mo/Fe ratio of 14 (**1-Fe**) and 12 (**2-Fe**) was investigated using an acoustic levitator. After preparation of the slurries, a droplet with a volume of about 4 μL was immediately injected in the acoustic levitator. The drying process took about 30 min and was monitored simultaneously with X-ray scattering and Raman spectroscopy. The change of the droplet volume in relation to levitation time had been followed.

The corresponding series of in situ Raman spectra collected during the acoustic levitation are presented in Figure 2.

The spectrum of **1-Fe** sample changed during the drying process, whereas in principle no alterations were observed for the **2-Fe** sample. The band at 1048 cm^{-1} results from NO_3^- anions.[13] For characterizing the nature of molybdate anionic species the position of the characteristic terminal Mo═O band has to be inspected. It is known from the literature[14] and our own measurements that the band position of ν_s(Mo−O_t) in the 990−940 cm^{-1} spectral range shifts to higher wavenumbers with decreasing pH value and, consequently, increasing condensation degree of the molybdate ions. In addition, the incorporation of other metal ions into the molybdate anions can cause a band shift, too. Thus, it was described that the

dx.doi.org/10.1021/cm202674f | Chem. Mater. 2011, 23, 5425−5431

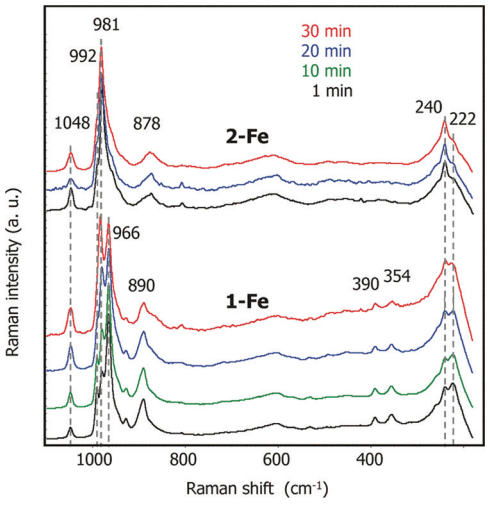

Figure 2. In situ Raman spectra collected during the drying process of samples **1-Fe** and **2-Fe** in a levitated droplet.

ν_s(Mo−O_t) band position of different Anderson-type $(NH_4)_3[XMo_6O_{24}H_6]\cdot 7H_2O$ phases changes in dependence on X from 944 cm^{-1} (Al) to 948 cm^{-1} (Ga) and 957 cm^{-1} (Fe).[15] Our own measurements of ammonium containing molybdate solutions containing Ni^{2+}, Fe^{3+}, and Bi^{3+} ions showed the following shift of the characteristic terminal Mo═O band: $[Mo_7O_{24}]^{6-}$ (939 cm^{-1}) → $[MMo_6O_{24}]^{3-}$ (939−957 cm^{-1}) → $[Mo_8O_{26}]^{4-}$ (965−970 cm^{-1}) → $[PMo_{12}O_{40}]^{3-}$ (978−993 cm^{-1}).[17b] In parallel, the respective bands of bridging ν(Mo−O) vibrations shift from 210−220 cm^{-1} ($[Mo_7O_{24}]^{6-}$/$[Mo_8O_{26}]^{4-}$) to 240 cm^{-1} ($[PMo_{12}O_{40}]^{3-}$). For Keggin-type $[XM_{12}O_{40}]^{n-}$ anions (X = B^{3+}, Si^{4+}, Ge^{4+}, P^{5+}, As^{5+}; M = Mo, W) it was found that X as well as the countercation could influence the position of the terminal Mo═O band.[16] These results are displayed in Figure 3.

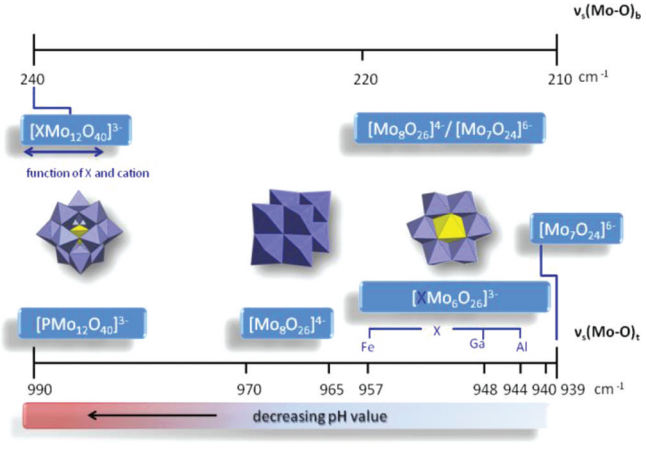

Figure 3. Raman shifts of oxomolybdate compounds of different complexity relevant for this study.

Taking these findings into account it is obvious from the in situ Raman spectra displayed in Figure 2 that two molybdate anions with different condensation degree exist in sample **1-Fe** (terminal Mo═O: 981/966 cm^{-1}; bridging Mo−O−Mo: 240/222 cm^{-1}). These anions are observable in sample **2-Fe**, too; however, the intensity ratios of the terminal Mo═O bands differ distinctly. It is evident, that the formation of Keggin-type $[PMo_{12}O_{40}]^{3-}$ anions (Mo═O band at 981 cm^{-1}) is favored in sample **2-Fe**.

In sample **1-Fe** the Keggin-type anions are enriched during the drying process. As can be seen from the in situ Raman spectra (Figure 2), the intensity ratios of the bands at 966 cm^{-1}/981 cm^{-1} vary from 1.9 after 1 min to 0.9 after 30 min levitation time. While the band at 981 cm^{-1} is clearly related to the Keggin-type molybdate ion, the assignment of the 966 cm^{-1} band seems to be not simple. The terminal Mo═O band position of an Anderson-type $[FeMo_6O_{24}H_6]^{3-}$ anion would be expected at 957 cm^{-1}.[15] Our own investigations of solutions containing only AHM, iron nitrate, and HNO_3 (Mo/Fe = 14:1) confirmed this. However, it was observed that after stirring this solution for 20 min at room temperature that the intensity of the band at 957 cm^{-1} decreased and a new one at 967 cm^{-1} appeared. This finding points to a progressive condensation of $[FeMo_6O_{24}H_6]^{3-}$ anions in the acidic solution. According to the band position the formation of octamolybdate anions can be assumed. Therefore, the band at 966 cm^{-1} which is observed during drying of sample **1-Fe** is assigned to such octamolybdate species.

Whereas some insights into the drying process on the molecular scale were obtained with Raman spectroscopy, long-range order phenomena like crystallization has been investigated with the X-ray diffraction measured simultaneously.

The X-ray scattering results for the higher Mo/Fe ratio (**1-Fe**) are presented in Figure 4. Directly after the start of drying

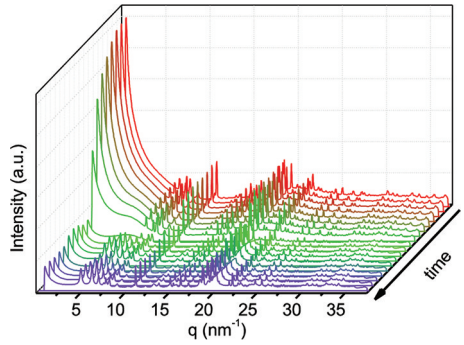

Figure 4. Diffraction patterns of sample **1-Fe** collected during the 30 min drying process in a levitated droplet.

process, Bragg reflections appeared which indicate the presence of at least one crystalline phase. After 20 min the formation of a further phase revealed.

The diffraction patterns were carefully corrected for amorphous background contributions before phase analysis. This analysis denoted the existence of two different phases at the beginning of the experiment. The diffraction pattern of one of these compounds was indexed to a cubic crystal system with the lattice constant a = 11.666 Å. The obtained data coincide with the PDF database entry 09-412 of $(NH_4)_3PO_4(MoO_3)_{12}\cdot 4H_2O$ (JCPDS-ICCD, Joint Committee on Powder Diffraction International Centre for Diffraction Data). The diffraction pattern of the second phase could be assigned to $(NH_4)Fe_3P_6O_{20}\cdot 10H_2O$ (PDF 31-053). After 20 min of drying a further crystalline phase evolved, which could be assigned to a second orthorhombic Keggin phase isostructural to $H_3PW_{12}O_{40}(H_2O)_{21}$ (PDF 70-705, JCPDS-ICCD). The formation of this second phase correlated with the increasing intensity of the Raman band typical for the Keggin

dx.doi.org/10.1021/cm202674f | Chem. Mater. 2011, 23, 5425−5431

anion. In contrast, no hints for a phosphate phase like $(NH_4)Fe_3P_6O_{20}{\cdot}10H_2O$ (PDF 31-053) were found in the Raman spectra. This is not surprising since the Raman band for the phosphate ion should be observable in the sane range between 900 and 1000 cm^{-1} like the intense M−O vibrations and can only be detected for high phosphate concentrations. Hence, such significant bands for phosphate clearly distinguishable from the M═O vibrations cannot be expected in our Raman investigations. Whereas an octamolybdate anion was clearly detectable with Raman spectroscopy, no octamolybdate containing phase could be observed by XRD. An obvious interpretation is that these anions formed an X-ray amorphous phase and can therefore not be detected. These results confirm the advantageous complementary of both methods used for this investigations.

As expected because of the Raman results, the Keggin phase with the cubic crystal system dominates the diffraction patterns obtained for **2-Fe** with the higher Fe content from the beginning until the end of the drying process. Surprisingly, during the experiment a spatial phase separation was observed. Scanning experiments, where the droplet was moved through the micro beam of X-rays, revealed the formation of two distinct parts of crystallization products. In the lower part of the droplet only the formation of the cubic Keggin phase could be observed. The upper part of the droplet consisted of probably three additional crystalline phases: the orthorhombic Keggin phase, the phosphate $(NH_4)Fe_3P_6O_{20}{\cdot}10H_2O$, and a further phase which could not be assigned to a known structure. Comparison with the Raman spectra which detected the entire droplet volume suggests that this phase consisted of octamolybdate anions which were observed with Raman spectroscopy as a minor component.

Further insights into the particle growth and morphology are available from the evaluation of the scattering curves at small angles. It has to be kept in mind that the setup chosen for the presented experiments and the nature of the specimen (far from a diluted system) constrains the information available in the SAXS regime. Furthermore it must be noted that a straightforward SAXS evaluation usually relies on dispersed noninteracting solutions of monodispersed particles. During the synthesis considerable interparticle correlations must be considered, and the system is often poly disperse. In this case SAXS cannot be used solely to construct the composition, and therefore complementary information is needed. SEM measurements have therefore been utilized to verify the particle sizes obtained from scattering experiments. The resulting SAXS-SEM size determination led to higher accuracy than from SAXS experiments alone.

Nevertheless, the changes in the low q-range are in accordance with the observations regarding crystallization in the wide angle area of the scattering curve. Starting from a pronounced SAXS signal, which can be interpreted as the presence of approximately spherical particles, the signal diminished during the experiments to the same degree as the crystallization proceeds. An estimation of the crystallite size was possible for the final product of **2-Fe** and results in a diameter of about 50 nm. A comparison with the SEM image shows an agglomeration of particles which are slightly larger (60−100 nm). For the sample **1-Fe** SEM reveals nearly the same particle size (Figure 5 a and d).

In additional experiments the decrease of the volume during the drying process was monitored under comparable conditions (Figure 6). Such investigations allow the statement about the

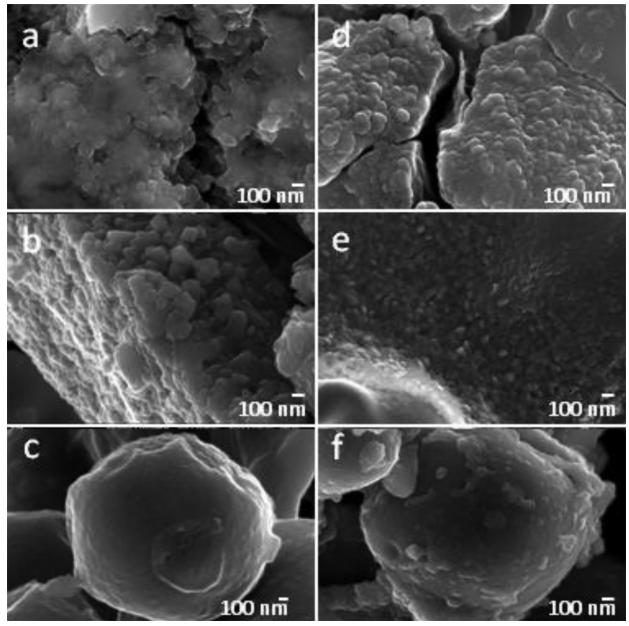

Figure 5. SEM pictures of dried samples **1-Fe**(a−c) and **2-Fe**(d−f) obtained via different preparation methods; panels a,d, ultrasonic levitation; panels b,e, spray drying; and panels c, f, filtration.

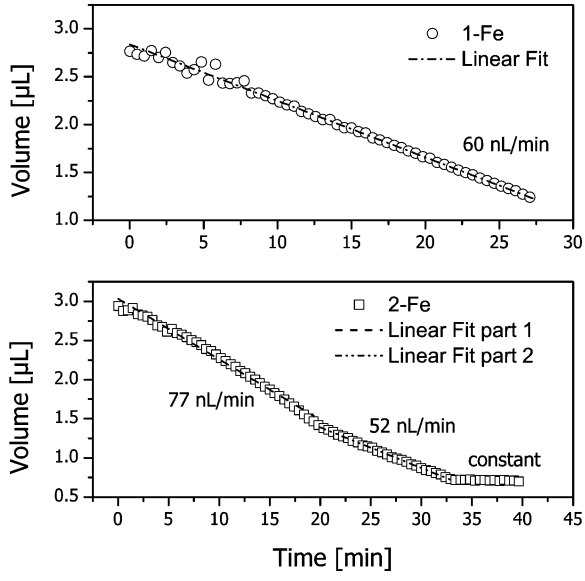

Figure 6. Decrease of the droplet volume during the drying process of samples **1-Fe** and **2-Fe**.

sublimation of water during the process. Whereas for **1-Fe** a linear decrease of the droplet volume with a slope of 60 nL/min could be observed, three distinct regions depending on the time could be found for **2-Fe**. Until 20 min the volume changes with 77 nL/min, then the changes of the volume is decelerated (52 nL/min) and after 33 min the volume remains constant. It could be proposed that the observed phase separation influences the volume change and led to this behavior.

The main objective of this study was to check if the concept of levitated droplets is a suitable model for spray drying. For this purpose, the samples obtained from the experiments in the ultrasonic levitator were compared to those obtained by conventional spray drying experiments using the same starting material and, additionally, to the dried samples obtained by

dx.doi.org/10.1021/cm202674f | *Chem. Mater.* 2011, 23, 5425−5431

filtration using the precipitate from the slurry phase. In Table 1 the Mo/Fe ratios obtained with inductively coupled plasma optical emission spectroscopy (ICP-OES) are listed. As expected the measured Mo/Fe ratio for the spray dried samples match with the theoretical Mo/Fe amount. The same amount can be expected for the samples dried in the ultrasonic levitator. For the filtrated sample with the high Fe amount (**2-Fe**) only a slight difference between theoretical and measured ratio could be observed, whereas for the other sample (**1-Fe**) a large part of the Fe ions obviously remains in the solution after filtration. These differences between **1-Fe** and **2-Fe** coincide with the different structural composition of the two samples observed in the in situ drying experiments. In the following the influence of the different conditioning procedures on the phase structure is discussed.

Table 1. ICP-OES Results of Samples Obtained by Filtration and Spray Drying

sample	treatment	Mo/Fe theoretical	Mo/Fe measured
1-Fe	spray dried	14: 1	13.8: 1
	filtration		19.6: 1
2-Fe	spray dried	12: 1	11.5: 1
	filtration		11.0: 1

The Raman spectra of **1-Fe** and **2-Fe** solids obtained after drying the slurry in the ultrasonic levitator, after conventional spray drying, and after filtrating the precipitate and drying at room temperature are displayed in Figure 7. It can be seen that the respective spectra of the spray dried and levitated samples accord. As expected, the spectra of the dried isolated precipitates of **1-Fe** and **2-Fe** are not comparable and differ from the spectra of the respective dried slurry phases. The latter is understandable because the dried slurry phase represents the whole phase composition (liquid and precipitate) whereas the precipitate comprises only the deposited components. Obviously, the band at 965 cm^{-1} dominates the spectrum of the dried precipitate **1-Fe** whereas the band at 982 cm^{-1} has only low intensity. This indicates that the lower condensed molybdate species are enriched in the precipitate and the Keggin-type anions are mainly in the liquid phase of the slurry. A similar, less pronounced effect is also observed for the dried precipitate **2-Fe** which is all the more striking given that the compositions of the different dried samples are nearly the same. The results obtained for **1-Fe** after different conditioning procedures are in accordance with the results previously described suggesting, that the Mo/Fe ratio determines the phase composition. Additionally, the drying procedure influences the structures obtained after drying as shown clearly by the results obtained for **2-Fe**.

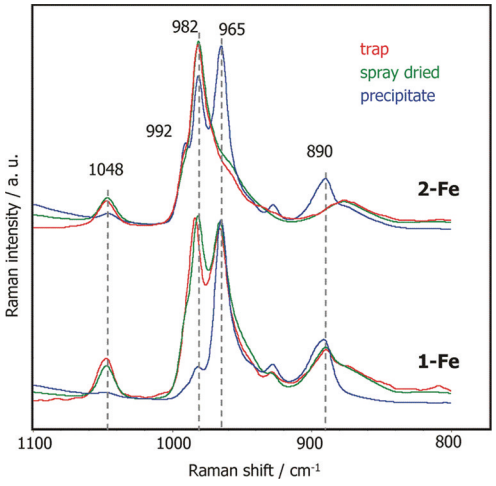

Figure 7. Raman spectra of the dried samples **1-Fe** and **2-Fe** obtained via three different preparation methods.

Normally, a more or less intensive Raman band of the phosphate ion is observable in the range of 900−1000 cm^{-1}. Thus we found the ν P−O bands for H_3PO_4 (85%) at 900 cm^{-1}, for $NH_4MnPO_4{\cdot}H_2O$ at 941 cm^{-1}, and for a 2 molar aqueous solution of $(NH_4)_2HPO_4$ at 988 cm^{-1}. However, the latter band was no more detectable in a 0.2 molar $(NH_4)_2HPO_4$ solution. Thus, it is difficult to observe phosphate bands in presence of molybdate anions in the Raman spectra. This problem can be overcome by measuring the respective ATR-FTIR spectra which provide additional information on the nature of phosphate species.[17] The ATR-FTIR spectra of the spray dried samples and the dried precipitates **1-Fe** and **2-Fe** are shown in Figure 8. Besides the M═O bands around 940 cm^{-1} several phosphate bands between 1015−1062 cm^{-1} can be seen in all samples. The band at 1062 cm^{-1} results from the phosphate in the Keggin $[PMo_{12}O_{40}]^{3-}$ anion.[18] The other bands at 1038 and 1017 cm^{-1} represent different additional phosphate ions. This finding leads to the conclusion that pure iron phosphate or ammonium iron phosphate phases were formed besides ammonium molybdate phases. From the well resolved phosphate bands in the precipitate samples it is clearly seen that in contrast to sample **2-Fe** almost no Keggin-phase is formed in the **1-Fe** sample which agrees well with the respective Raman measurements. Because of the overlapping phosphate bands in the spray dried samples a detailed discussion is challenging.

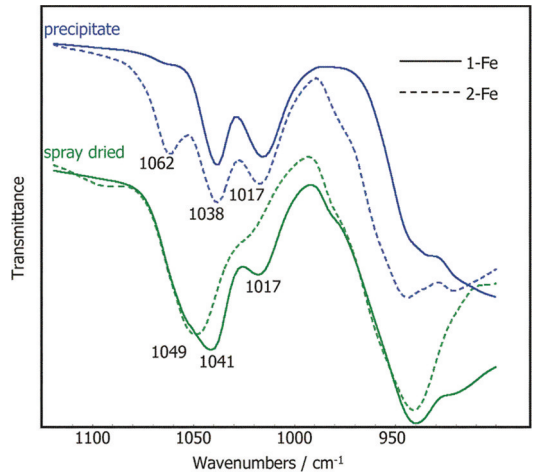

Figure 8. FTIR spectra of the dried samples **1-Fe** and **2-Fe** obtained via different preparation methods.

The diffraction patterns presented in Figure 9 confirm the observations obtained by Raman spectroscopy (Figure 7). The patterns of the spray dried samples and the precipitate reflect the differences obtained for the molecular anions by Raman and attenuated total reflection (ATR-IR) spectroscopy. For the precipitate of **1-Fe** the $(NH_4)Fe_3P_6O_{20} \times 10\ H_2O$ phase (PDF 31-0053) could be observed. Additional reflections occurred which could be proposed as originated from an octomolybdate

dx.doi.org/10.1021/cm202674f | Chem. Mater. 2011, 23, 5425−5431

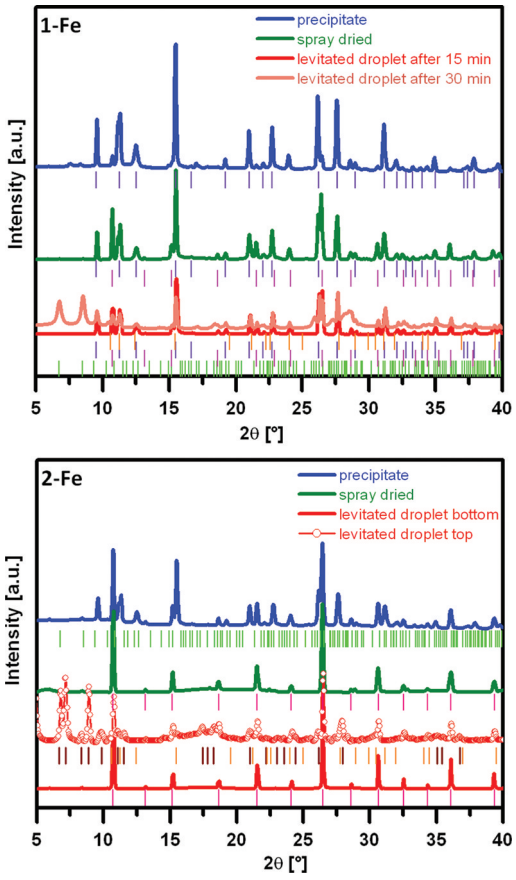

Figure 9. Diffraction patterns of the dried samples **1-Fe** and **2-Fe** obtained via different preparation methods and indexed Bragg reflections. (green, PDF 70-0705 orthorhombic Keggin structure; pink, PDF 70-0130 cubic Keggin structure; orange, PDF 31-0053 $(NH_4)Fe_3P_6O_{10}{\cdot}10H_2O$; brown and violet, probably octamolybdate phases.

containing phase. Next to these phases the cubic phase consisting of Keggin ions (PDF 09-412) could be found in the spray-dried sample. This pattern is similar to the ones obtained for the first 20 min in the ultrasonic levitator. The orthorhombic Keggin phase formed after 20 min drying in the levitator could not be found in the spray dried sample. The results obtained for **2-Fe** are comparable to these findings obtained for **1-Fe**. The spray-dried sample consisted only of the cubic Keggin phase, whereas in the precipitate the phosphate- and probably the octamolybdate-containing phases were obtained. The spray dried sample had the same structural composition like the levitated droplet at the beginning of the drying. The phases formed after about 20 min in the top of the droplet could not be found in the spray-dried sample. Thus, it can be concluded, that the first minutes of the drying of the levitated droplets match the processes during the spray drying under our conditions. Probably, the phases found at the end of the drying in the ultrasonic levitator could be also obtained after spray-drying under more moderate conditions.

As SEM investigations (Figure 5) reveal, the morphology of the particles obtained after spray-drying and after the levitation was similar, whereas the precipitate consisted of large particles with a multitude of smaller crystallites. Remarkably, the crystallite size for all samples estimated from the FWHM of the Bragg reflections is in the same order between 50 and 70 nm.

CONCLUSIONS

The coupling of Raman spectroscopy and X-ray scattering allows detailed structural insights into the dynamic processes during the drying and crystallization from the atomic up to the nanometer scale. The results presented in this work suggest that the approach used to monitor the structural changes during the spray drying with investigations at levitated droplets is promising. It could be demonstrated that the samples obtained by drying in an acoustic levitator and by spray drying show no significant differences, whereas the solids isolated by filtration and following drying show another phase composition. The SEM images reveal that the morphologies of the samples and their crystallite sizes are comparable. Additional volume measurements offer the possibility for a kinetic modeling of the drying process. Thus, a knowledge-based optimization of crystallization processes in terms of tailoring phase compositions and particle sizes seems to be possible.

AUTHOR INFORMATION

Corresponding Author

*E-mail: joerg.radnik@catalysis.de (J.R.), franziska.emmerling@bam.de (F.E.).

ACKNOWLEDGMENTS

The authors are grateful to S. Benemann for providing the SEM images. We thank L. R. Knöpke (LIKAT) and the BESSY staff, especially I. Zizak for technical support.

REFERENCES

(1) (a) Lin, M. M. *Appl. Catal., A* **2003**, *250* (2), 287. (b) Boissiere, C.; Grosso, D.; Amenitsch, H.; Gibaud, A.; Coupe, A.; Baccile, N.; Sanchez, C. *Chem. Commun.* **2003**, No. 22, 2798.

(2) (a) Iskandar, F.; Mikrajuddin.; Okuyama, K. *Nano Lett.* **2001**, *1* (5), 231. (b) Iskandar, F.; Mikrajuddin.; Okuyama, K. *Nano Lett.* **2002**, *2* (4), 389. (c) Le, M. T.; van Well, W. J. M.; van Driessche, I.; Hoste, S. *Appl. Catal., A* **2004**, *267* (1−2), 227.

(3) Hergeth, W. D.; Jaeckle, C.; Krell, M. *Polym. React. Eng.* **2003**, *11* (4), 663.

(4) Sen, D.; Spalla, O.; Tache, O.; Haltebourg, P.; Thill, A. *Langmuir* **2007**, *23* (8), 4296.

(5) (a) Schiffter, H.; Lee, G. *J. Pharm. Sci.* **2007**, *96* (9), 2274. (b) Schiffter, H.; Lee, G. *J. Pharm. Sci.* **2007**, *96* (9), 2284. (c) Sloth, J.; Kiil, S.; Jensen, A. D.; Andersen, S. K.; Jorgensen, K.; Schiffter, H.; Lee, G. *Chem. Eng. Sci.* **2006**, *61* (8), 2701.

(6) (a) Delissen, F.; Leiterer, J.; Bienert, R.; Emmerling, F.; Thünemann, A. F. *Anal. Bioanal. Chem.* **2008**, *392* (1−2), 161. (b) Wolf, S. E.; Leiterer, J.; Kappl, M.; Emmerling, F.; Tremel, W. *J. Am. Chem. Soc.* **2008**, *130* (37), 12342.

(7) (a) Polte, J.; Emmerling, F.; Radtke, M.; Reinholz, U.; Riesemeier, H.; Thunemann, A. F. *Langmuir* **2010**, *26* (8), 5889. (b) Polte, J.; Ahner, T. T.; Delissen, F.; Sokolov, S.; Emmerling, F.; Thunemann, A. F.; Kraehnert, R. *J. Am. Chem. Soc.* **2010**, *132* (4), 1296. (c) Klimakow, M.; Leiterer, J.; Kneipp, J.; Rossler, E.; Panne, U.; Rademann, K.; Emmerling, F. *Langmuir* **2010**, *26* (13), 11233.

(8) Leiterer, J.; Emmerling, F.; Radnik, J.; Bentrup, U.; Bruckner, A. *Catal. Today* **2010**, *155* (3−4), 326.

(9) (a) Leiterer, J.; Emmerling, F.; Panne, U.; Christen, W.; Rademann, K. *Langmuir* **2008**, *24* (15), 7970. (b) Wolf, S. E.; Leiterer, J.; Kappl, M.; Emmerling, F.; Tremel, W. *J. Am. Chem. Soc.* **2008**, *130*, 12342.

(10) Paris, O.; Li, C.; Siegel, S.; Weseloh, G.; Emmerling, F.; Riesemeier, H.; Erko, A.; Fratzl, P. *J. Appl. Crystallogr.* **2007**, *40* (s1), S466.

(11) Hammersley, A. P.; Svensson, S. O.; Hanfland, M.; Fitch, A. N.; Hausermann, D. *High Pressure Res.* **1996**, *14* (4−6), 235.

(12) Leiterer, J.; Delissen, F.; Emmerling, F.; Thunemann, A. F.; Panne, U. *Anal. Bioanal. Chem.* **2008**, *391* (4), 1221.
(13) Nakamoto, K. *Infrared and Raman spectra of inorganic and coordination compounds, Part A*; John Wiley & Sons, Inc.: New York, 1997.
(14) Griffith, W. P.; Lesniak, P. J. B. *J. Chem. Soc., A* **1969**, No. 7, 1066.
(15) Botto, I. L.; Garcia, A. C.; Thomas, H. J. *J. Phys. Chem. Solids* **1992**, *53* (8), 1075.
(16) (a) Rocchicciolideltcheff, C.; Fournier, M.; Franck, R.; Thouvenot, R. *Inorg. Chem.* **1983**, *22* (2), 207. (b) Rocchicciolideltcheff, C.; Thouvenot, R.; Franck, R. *Spectrochim. Acta, Part A* **1976**, *32* (3), 587.
(17) (a) Bentrup, U. *Chem. Soc. Rev.* **2010**, *39* (12), 4718. (b) Bentrup, U.; Radnik, J.; Armbruster, U.; Martin, A.; Leiterer, J.; Emmerling, F.; Bruckner, A. *Top. Catal.* **2009**, *52* (10), 1350.
(18) Fournier, M.; Thouvenot, R.; Rocchicciolideltcheff, C. *J. Chem. Soc., Faraday Trans.* **1991**, *87* (2), 349.